Low-lying dipole excitations in the odd-proton, midshell nucleus ^{103}Rh

F. Stedile,[1] E. Fill,[2] D. Belic,[1] P. von Brentano,[3] C. Fransen,[3] A. Gade,[3] U. Kneissl,[1] C. Kohstall,[1] A. Linnemann,[3] P. Matschinsky,[3] A. Nord,[1,*] N. Pietralla,[3,†] H. H. Pitz,[1] M. Scheck,[1] and V. Werner[3]
[1]*Institut für Strahlenphysik, Universität Stuttgart, Allmandring 3, D-70569 Stuttgart, Germany*
[2]*Max-Planck-Institut für Quantenoptik, D-85748 Garching, Germany*
[3]*Institut für Kernphysik, Universität zu Köln, Zülpicher Str. 77, D-50937 Köln, Germany*
(Received 31 August 2000; published 24 January 2001)

Low-lying dipole excitations in the odd-proton, midshell nucleus ^{103}Rh were investigated in photon scattering experiments at the Stuttgart Dynamitron facility using bremsstrahlung beams with end point energies of 4.1 and 2.4 MeV. In total, 106 excited levels, most of them unknown so far, could be observed in the excitation energy range from 1.2 to 4.0 MeV. In addition to 106 transitions to the ground state ($J_0^\pi = 1/2^-$), 20 transitions to the low-lying $J^\pi = 3/2^-$ level at 295 keV and 10 transitions to the $J^\pi = 5/2^-$ state at 357 keV were detected. For 20 photoexcited levels spins could be suggested from the measured angular distribution data. The reduced ground-state transition strengths summed up in the energy range 2–4 MeV amount to $\Sigma g\Gamma_0^{\mathrm{red}} = (16.3 \pm 1.9)$ meV/MeV^3 corresponding, under the assumption of an electric character for all excitations, to a total excitation strength of $\Sigma B(E1)\uparrow = (15.6 \pm 1.8) \times 10^{-3}\ e^2\,\mathrm{fm}^2$. The fragmentation of the dipole strength and the decay branchings of the photoexcited levels are discussed. The observed feedings of the 295 and 357 keV levels result in a population inversion, the precondition for a possible γ-ray laser.

DOI: 10.1103/PhysRevC.63.024320 PACS number(s): 25.20.Dc, 21.10.Re, 23.20.−g, 27.60.+j

I. MOTIVATION

The nucleus ^{103}Rh has 45 protons and 58 neutrons and hence lies in a mass region rather far from the shell closures at $Z = 50$ and $N = 50$, but, on the other hand, is also outside the islands of well deformed nuclei [1]. Therefore, the exploration and explanation of the excitation scheme of this odd-mass transitional, midshell nucleus represents a real challenge for nuclear structure studies due to its complicated diverse excitation possibilities and the various applicable model interpretations.

The isotope ^{103}Rh exhibits an interesting low-energy level scheme. Only about 40 keV above the stable ground state ($J_0^\pi = 1/2^-$) a long-lived isomer occurs ($J^\pi = 7/2^+$, $T_{1/2} = 56.1$ min). On top of this isomeric state a nearby $9/2^+$ level exists at an excitation energy of 93 keV. The next excited states are the $3/2^-$ and $5/2^-$ levels at 295 and 357 keV, respectively, which considerably differ in their lifetimes τ (9.7 and 107 ps). Nearly identical level schemes were observed in the neighboring, unstable $N = 58$ isotone ^{105}Ag and the stable, odd-mass Ag isotopes ^{107,109}Ag [2]. This observation is a clear hint to common low-energy structures and excitations in these odd-mass nuclei.

Early Coulomb excitation experiments on ^{103}Rh and ^{107,109}Ag in 1954 by Heydenburg and Temmer [3] ascribed the spins $3/2^-$ and $5/2^-$ to the two higher-lying levels discussed above. These levels together with the $1/2^-$ ground state were interpreted as a $K = 1/2^-$ rotational band by these authors. Later reorientation precision measurements of the quadrupole moments of the $3/2^-$ and $5/2^-$ states in ^{103}Rh by Gelberg *et al.* [4] provided evidence for negative quadrupole moments. Their results could well be explained by these authors within a particle-core excitation model where the core was described by an interacting boson Hamiltonian [5]. Sayer *et al.* [6] interpreted in 1972 their Coulomb excitation results in terms of a core-excitation model by the coupling of a $p_{1/2}$ proton to an even-even ^{102}Ru core. Subsequent (γ-γ)-directional correlation data obtained by Bargholtz *et al.* [7] could be explained successfully within the framework of a unified vibrational model [8,9].

The negative quadrupole moments observed by Gelberg *et al.* [4] and hence the expected oblate ground-state deformation easily explain the ground-state spin of $1/2^-$ and the existence of the low-lying, long-lived $7/2^+$ isomer since in the Nilsson level scheme for protons [10] a unique, isolated crossing of the orbits 1/2[301] and 7/2[413], expected for the 45th proton, occurs at a negative deformation parameter of about $\epsilon_2 \approx -0.122$ (corresponding to a deformation parameter of $\delta \approx -0.125$). Furthermore, investigations of the electric giant dipole resonance (GDR) of ^{103}Rh in (γ,xn) cross section measurements [11] showed a slight deformation splitting of the GDR. Somewhat better fits to the broadened GDR shape could be achieved by fitting with two Lorentzians, indicating a nonzero deformation of ^{103}Rh. Unfortunately, at this time the fits were performed with the constraint of a prolate deformation to avoid too many degrees of freedom in the fitting procedure. However, it seems to be possible to describe the broadened GDR of ^{103}Rh also by assuming a slightly oblate deformation.

The aim of the present photon scattering experiments was twofold. First of all, it was of interest to study the fragmentation of low-lying dipole strength in this odd-mass, transitional nucleus. As is well known, in even-even nuclei various enhanced dipole modes occur. Outstanding examples are

*Present address: Agilent Technologies Deutschland, D-71034 Böblingen, Germany.
†Present address WNSL, Yale University, New Haven, CT 06520-8124.

the orbital $M1$ excitations in deformed nuclei, the so-called scissors mode [12] (for a compilation of data see, e.g., Ref. [13]) or the $E1$ two-phonon excitations to the $J^\pi=1^-$ member of the quintuplet built by the coupling of the 2^+ and 3^- phonons. Such excitations have been observed in the purest form in semimagic, spherical nuclei such as the $N=82$ isotones (see Ref. [14] and references therein) and the $Z=50$ tin isotopes [15]. The fragmentation of these common excitation modes in the neighboring odd-mass nuclei were extensively studied both experimentally and theoretically [16–27]. Also for more γ-soft nuclei such as the pair ^{134}Ba/^{133}Cs [28,29] or the vibrational nuclei of the Cd isotopic chain [30,31] the fragmentation of the dipole strength was studied in systematic photon scattering experiments at the Stuttgart Dynamitron facility [13]. Therefore, it was of interest to investigate this medium-heavy, transitional nucleus ^{103}Rh in sensitive photon scattering experiments especially since this nucleus has been studied so far only in rather crude, low-energy photon scattering experiments ($E_\gamma \leqslant 1.65$ MeV) [32] in 1981, where only two photoexcited states at 803 and 1277 keV could be detected.

Another attractive feature of the low-energy level scheme of ^{103}Rh is the existence of the two levels at 295 and 357 keV, where the upper one has a considerably longer lifetime of 107 ps as compared to 9.7 ps for the lower one. This situation represents a promising condition to generate a population inversion of excited nuclear states via the feeding from a higher-lying photoexcited level. Therefore, an additional aim of the present study was the search for such a population inversion by photopumping which is the precondition for a pumping scheme in view of a possible γ-ray laser [33–36].

II. EXPERIMENTAL METHOD

A. The nuclear resonance fluorescence technique

Photon scattering off bound states, nuclear resonance fluorescence (NRF), represents the most sensitive technique to study low-lying dipole excitations in heavy nuclei, both of electric and magnetic character (Ref. [13] and references therein). Precise excitation energies E_x, ground-state transition widths Γ_0, but also decay branching ratios R can be extracted from the spectra of the scattered photons measured in NRF experiments. These quantities can be converted into reduced transition probabilities $B(E1)\uparrow$, $B(M1)\uparrow$, or lifetimes τ. For nuclear structure investigations additionally model independent information on the spins and parities of the photoexcited levels can be deduced from angular distribution and linear polarization measurements, respectively (in the favorable cases of even-even nuclei). The formalism describing photon scattering experiments is outlined in more detail in previous reviews [13,37].

In experiments using continuous bremsstrahlung as a photon beam one automatically integrates over the resonances. Therefore, the integrated scattering cross sections, the scattering intensities, are measured. The total scattering intensity $I_{S,f}$ for a decay of the photoexcited state to a final level labeled by f, integrated over the full solid angle, is given by

$$I_{S,f}=g\left(\pi\frac{\hbar c}{E_\gamma}\right)^2\frac{\Gamma_0\Gamma_f}{\Gamma}, \tag{1}$$

where Γ_0, Γ_f, and Γ are the decay widths of the photoexcited state with spin J to the ground state (spin J_0), to a final lower-lying state (spin J_f) and its total width, respectively. The statistical weight $g=(2J+1)/(2J_0+1)$ is called the ''spin factor.'' The product $g\Gamma_0$ can be directly extracted from the measured scattering intensities. It is proportional to the reduced excitation probabilities $B(E1)\uparrow$ or $B(M1)\uparrow$:

$$B(\Pi 1)\uparrow = g\,B(\Pi 1)\downarrow = \frac{9}{16\pi}\left(\frac{\hbar c}{E_\gamma}\right)^3 (g\Gamma_0) \tag{2}$$

and in numerical form

$$B(E1)\uparrow = 0.955\,\frac{g\Gamma_0}{E_\gamma^3}\,[10^{-3}\ \ e^2\,\mathrm{fm}^2] \tag{3}$$

$$B(M1)\uparrow = 0.0864\,\frac{g\Gamma_0}{E_\gamma^3}\,[\mu_N^2], \tag{4}$$

where the excitation energies E_x should be taken in MeV and the ground-state transition widths Γ_0 in meV.

Unfortunately, in the case of odd-mass target nuclei the angular distributions of the scattered photons are rather isotropic. Therefore, in general, except for the favorable case of a ground-state spin $J_0=1/2$ and strong transitions (see Sec. III), no unambiguous spin assignments to the photoexcited states are possible in present day experiments and hence the spin factor g is unknown. It should be mentioned that the vanishing anisotropy in the angular distributions in addition leads to rather low polarizations of the scattered photons. This implies that also no parity assignments are possible by polarization measurements as in the case of even-even nuclei.

For the comparison with the strengths in even-even nuclei we introduce the quantity $g\Gamma_0^{\mathrm{red}}$:

$$g\Gamma_0^{\mathrm{red}} = g\,\frac{\Gamma_0}{E_\gamma^3}, \tag{5}$$

which is proportional to the reduced dipole excitation probabilities [see Eqs. (3) and (4)].

The decay branching ratios of the photoexcited states $R_{j,k}^{\mathrm{expt}}$ to lower-lying states labeled by j,k are defined as the ratio of the corresponding reduced transition probabilities

$$R_{j,k}^{\mathrm{expt}} = \frac{B(\Pi L;\,J\rightarrow J_j)}{B(\Pi L;\,J\rightarrow J_k)} = \frac{\Gamma_j}{\Gamma_k}\,\frac{E_{\gamma k}^3}{E_{\gamma j}^3}. \tag{6}$$

The branching ratios contain, in particular in the case of deformed nuclei, valuable information on the spin J of the photoexcited state (for known spins J_j and J_k). Furthermore, the K quantum number of the photoexcited state can be extracted within the validity of the Alaga rules [38].

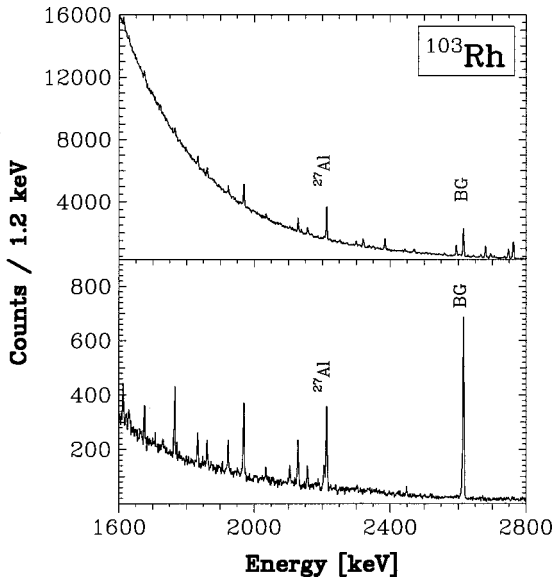

FIG. 1. Spectra of photons scattered off ^{103}Rh, measured at a scattering angle of 127° using bremsstrahlung beams of endpoint energies of 4.1 MeV (upper part) and 2.4 MeV (lower part), respectively. Calibration lines (^{27}Al), and background lines (BG: ^{208}Pb) are marked (see text).

B. Experimental setup

The present NRF experiments on ^{103}Rh were performed at the bremsstrahlung facility of the Stuttgart Dynamitron accelerator [13,17]. Two measurements at bremsstrahlung end point energies of 4.1 and 2.4 MeV were carried out to achieve an optimal sensitivity in a broad range of excitation energies, and to enable the detection of decay branching ratios. The dc electron currents used in the present experiments had to be limited, due to the thermal capacity of the radiator target, to about 250 μA. The scattering target consisted of high purity, monoisotopic, metallic Rh with a total mass of 2.950 g sandwiched by ^{27}Al discs (0.510 g; diameter 16 mm), serving for the photon flux calibration [39]. The scattered photons were detected by three high-resolution Ge γ-ray spectrometers installed at angles of about 90°, 127°, and 150° with respect to the incoming bremsstrahlung beam. The efficiencies of all three detectors amounted to about 100% each, relative to a standard 7.6 cm×7.6 cm NaI(Tl) detector. The energy resolution was typically about 2 keV at a photon energy of 1.3 MeV and about 3 keV at 3 MeV. The total effective time of data collection was about 140 h.

III. RESULTS

A. Spectra of photons scattered off ^{103}Rh, observed excitation strengths

Figure 1 shows the spectra of photons scattered off ^{103}Rh detected under a scattering angle of 127°. In the upper part the spectrum is depicted as measured using a bremsstrahlung beam of an end point energy of 4.1 MeV. In the lower part the corresponding spectrum for an end point energy of 2.4 MeV is shown. In both spectra the photon flux calibration lines (^{27}Al) and the background lines (BG) stemming from natural environmental activity (^{208}Pb) are marked. All other peaks correspond to transitions in ^{103}Rh. The comparison of both spectra clearly documents the considerably enhanced peak-to-background ratio in the lower spectrum taken at a reduced end point energy of 2.4 MeV. This allows us to detect and to identify inelastic transitions and to measure branching ratios of higher-lying levels with improved sensitivity.

One of the main goals of the present experiments was the study of the populations of the two low-lying levels in ^{103}Rh at 295 and 357 keV (see inset of Fig. 2) by feeding from higher-lying photo-excited levels. These two levels with spins $J_1^\pi = 3/2^-$ and $J_2^\pi = 5/2^-$ differ considerably in their lifetimes (9.7 and 107 ps). Since the higher-lying level has the substantially longer lifetime, the nucleus ^{103}Rh seems to be a good candidate to search for a population inversion of excited nuclear states, the precondition for a pumping scheme of a possible γ-ray laser [33–36]. In the present experiments several strongly photoexcited levels could be detected, which show a considerable feeding of the two abovementioned low-lying levels of interest. This is shown exemplarily in Fig. 2. Here a section of the spectrum of scattered photons (end point energy 4.1 MeV) is depicted together with a simplified low-energy level scheme of ^{103}Rh

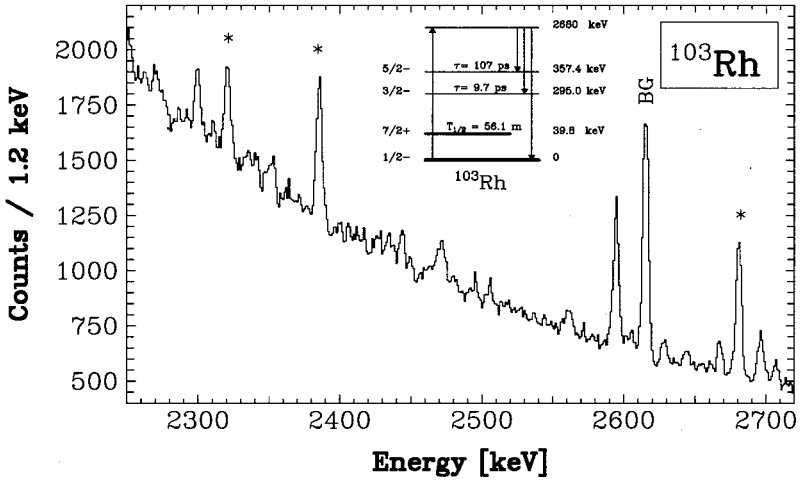

FIG. 2. Part of the ^{103}Rh(γ,γ') spectrum acquired using bremsstrahlung of an end point energy of 4.1 MeV. A background peak (2.614 MeV transition in ^{208}Pb) is labeled (BG). All other peaks are due to transitions in ^{103}Rh. Peaks exemplarily marked by asterisks correspond to the ground-state transition of a level at 2680 keV, which considerably feeds the two low-lying states at 295 and 357 keV, respectively, and the two corresponding feeding transitions. The inset shows the simplified low-energy level scheme of ^{103}Rh and the decay branching of the 2680 keV level.

(see inset). The strong peak at 2680 keV (marked by an asterisk) corresponds to the ground-state transition of a photoexcited level which exhibits a strong feeding to both levels (at 295 and 357 keV, respectively). The corresponding inelastic feeding transitions of 2385 and 2323 keV are also marked by asterisks. The measured decay branchings are discussed in more detail in Sec. IV B.

The results are summarized in numerical form in Table I. The quoted quantities are the excitation energies E_x (with an estimated total uncertainty of $\leqslant 1$ keV), the integrated scattering intensities $I_{S,0}$, the products $g\Gamma_0$ of the spin factor and the ground-state transition width, and the products $g\Gamma_0^{\mathrm{red}}$ of the spin factor and the reduced ground-state transition width. These quantities were converted into the reduced excitation widths $B(E1)\uparrow$ and $B(M1)\uparrow$ using Eqs. (3) and (4). These values are given in the last columns. If no decay branching was observed in the present experiment exclusive ground-state transitions of the photoexcited levels were assumed ($\Gamma_0=\Gamma$). Since spins $J>1/2$ of the excited states, mixing ratios δ and parities could not be determined unambiguously, an isotropic angular distribution of the scattered photons was assumed in the analysis and the reduced excitation probabilities are given for dipole excitations of both electric and magnetic character.

B. Decay branchings

γ-ray decay branchings were identified from the measured γ-singles data on the basis of the Ritz combination principle. In Table II the results are summarized for observed decay branchings of the photoexcited states in ^{103}Rh. Given are the level energies E_x, the total photon scattering intensities for decays to the ground state ($I_{S,0}$), to the excited level at 295 keV ($I_{S,1}$), and to the excited level at 357 keV ($I_{S,2}$). Furthermore, the corresponding decay branching ratios $R_{1,0}^{\mathrm{expt}}$ and $R_{2,0}^{\mathrm{expt}}$ are given. As can be seen from Table II there are four levels at 1969, 2680, 2801, and 3820 keV, which show a considerable feeding of both states of interest at 295 and 357 keV, respectively. A direct population of the lowest-lying excited state in ^{103}Rh, the long-lived isomer ($T_{1/2}=56.1$ min, $J^{\pi}=7/2^{+}$) at 39.8 keV (see inset of Fig. 2) could not be observed.

C. Angular distributions

As already mentioned, spin assignments from angular correlation measurements in NRF experiments are very difficult in the case of odd-mass nuclei, due to the rather isotropic angular distributions of the scattered photons. Only for isotopes with a ground-state spin $J_0=1/2$, as for ^{103}Rh, and for the favorable cases of strong transitions, enabling measurements with good statistics, some conclusions on the spin J of the photoexcited states can be drawn. In the present experiments the scattered photons were detected at only three scattering angles of 90°, 127°, and 150°, respectively. Therefore, in the analysis the intensity ratios $W(90°)/W(127°)$ and $W(90°)/W(150°)$ for ground-state transitions were deduced as detected by the various detectors (corrected for solid angles and relative efficiencies). In Fig. 3 the expected values of these ratios are plotted for different spins J together with the experimental results for states with probable spins $J=1/2$. Only these data are shown for the sake of clearness. For photoexcited states with $J=1/2$ the angular distribution of the scattered photons is exactly isotropic resulting in a value of 1 for both intensity ratios (shown as a full square in Fig. 3). For spins $J=5/2$, corresponding to pure electric quadrupole transitions, one expects the value shown in Fig. 3 by a full hexagon. In the case of $J=3/2$ the situation is more complicated. The expected intensity ratios strongly depend on the quadrupole/dipole mixing ratio δ resulting in the curve plotted in Fig. 3. The intensity ratios for some δ values, characterized by different symbols, are given in the inset of Fig. 3. In addition to the levels, to which a probable spin of $J=1/2$ was assigned, there are many others where a spin assignment of $J=3/2$ is probable, however, not unique. It should be mentioned, that, at least in principle, in the case of spin assignments $J=3/2$ and a finite mixing ratio δ a negative parity has to be allocated since a $E1/M2$ mixing can be excluded.

The data from the angular distribution measurements are summarized in Table III. Given are the excitation energies E_x, the intensity ratios $W(90°)/W(127°)$ and $W(90°)/W(150°)$ for ground-state transitions, and some tentative spin assignments in the last column. The ordering of the proposed spins is according to their probability. Unprobable assignments are given in brackets.

IV. DISCUSSION

A. Dipole strength distribution

Figure 4 shows the observed dipole strength distribution in ^{103}Rh. Plotted are the products of the spin factor g times the reduced ground-state decay widths Γ_0^{red} as a function of the excitation energy in the range of 1.2–4.0 MeV. The quantity $g\Gamma_0^{\mathrm{red}}$ is directly proportional to the reduced excitation probabilities [see Eqs. (3) and (4)]. Numerically $g\Gamma_0^{\mathrm{red}}=1$ meV/MeV^3 corresponds to $B(E1)\uparrow=0.955\times10^{-3}$ e^2 fm^2 or to $B(M1)\uparrow=0.0864$ μ_N^2. A strong fragmentation of the dipole strength is obvious with some concentration in two bumps around 2 and 2.7 MeV, respectively. Transition strengths marked by asterisks correspond to the excitation of levels which considerably feed both low-lying levels at 357 and 295 keV.

When investigating the total dipole strength and its fragmentation in odd-mass nuclei, the detection sensitivity is of crucial importance. The detection limits in the present photon scattering experiments are shown in Fig. 5. In this figure the minimal reduced ground-state transition width Γ_0^{red}, multiplied by the spin factor g, is plotted as a function of the excitation energy, needed for levels to be detected in the present experiments. The highest sensitivity in the experiment using a bremsstrahlung endpoint energy of 4.1 MeV can be reached for excitation energies around 3–3.5 MeV. The achieved value of $g\Gamma_0^{\mathrm{red}}\approx0.01$ meV/MeV^3 corresponds to $B(E1)\uparrow=0.955\times10^{-5}$ e^2 fm^2 or 0.864×10^{-3} μ_N^2. The reduced ground-state transition strengths summed up in the energy range 2–4 MeV amount to $\Sigma_{2-4\ \mathrm{MeV}}\ g\Gamma_0^{\mathrm{red}}=(16.3$

TABLE I. Numerical results for excitations observed in the reaction ^{103}Rh(γ,γ'): the excitation energies E_x, the integrated cross sections $I_{S,0}$, the ground-state transition widths $g\Gamma_0$, the reduced ground-state transition widths $g\Gamma_0^{\mathrm{red}}$, and the reduced excitation probabilities $B(M1)\uparrow$ and $B(E1)\uparrow$ are given.

E [keV]	$I_{S,0}$ [eV b]	$g\Gamma_0$ [meV]	$B(M1)\uparrow$ [μ_N^2]	$B(E1)\uparrow$ [10^{-3} e^2 fm^2]	$g\Gamma_0^{\mathrm{red}}$ [meV]/[MeV^3]
1277	2.31(24)	1.30(13)[a]	0.0541(55)	0.599(61)	0.626(64)
1614	1.04(20)	0.71(13)	0.0145(28)	0.160(31)	0.168(32)
1626	0.83(25)	0.57(17)	0.0114(35)	0.126(39)	0.132(40)
1778	0.98(18)	0.81(15)	0.0124(23)	0.137(25)	0.144(26)
1812	0.74(21)	0.63(18)	0.0092(26)	0.102(29)	0.107(30)
1861	2.41(23)	2.18(21)	0.0292(28)	0.323(31)	0.338(33)
1923	1.98(22)	2.97(31)	0.0361(37)	0.399(41)	0.418(43)
1943	0.73(16)	0.72(16)	0.0084(19)	0.093(21)	0.098(22)
1969	5.92(45)	9.83(63)	0.1113(71)	1.230(79)	1.288(82)
1997	0.94(18)	0.97(19)	0.0106(20)	0.117(23)	0.122(24)
2001	0.74(16)	0.77(17)	0.0083(19)	0.092(20)	0.096(21)
2034	1.15(18)	1.24(19)	0.0127(19)	0.140(21)	0.147(22)
2049	0.51(12)	0.56(13)	0.0057(13)	0.062(15)	0.065(15)
2059	0.93(18)	1.03(20)	0.0102(20)	0.113(22)	0.118(23)
2071	0.77(13)	0.86(15)	0.0084(14)	0.093(16)	0.097(17)
2075	1.03(14)	1.15(16)	0.0111(16)	0.123(17)	0.129(18)
2089	0.58(14)	0.66(16)	0.0063(15)	0.069(17)	0.073(18)
2128	4.64(36)	8.68(60)	0.0778(54)	0.861(60)	0.901(62)
2137	0.83(13)	0.99(15)	0.0088(14)	0.097(15)	0.101(16)
2155	2.17(24)	6.42(48)	0.0554(41)	0.612(46)	0.641(48)
2163	0.57(13)	0.69(16)	0.0059(14)	0.065(15)	0.069(16)
2196	0.52(14)	0.66(18)	0.0054(14)	0.059(16)	0.062(17)
2306	0.68(16)	0.94(23)	0.0066(16)	0.073(18)	0.077(19)
2319	2.91(29)	4.08(41)	0.0282(28)	0.312(31)	0.327(33)
2352	1.09(19)	1.57(28)	0.0104(19)	0.115(20)	0.120(21)
2362	0.58(12)	0.84(18)	0.0055(12)	0.061(13)	0.064(13)
2434	0.88(14)	1.35(22)	0.0081(13)	0.090(15)	0.094(15)
2463	0.53(12)	0.84(20)	0.0048(11)	0.054(12)	0.056(13)
2468	1.09(21)	3.50(44)	0.0201(25)	0.222(28)	0.233(29)
2478	0.40(11)	0.63(18)	0.0036(10)	0.040(11)	0.042(12)
2516	0.58(12)	3.53(47)	0.0191(25)	0.212(28)	0.222(29)
2544	0.53(11)	0.89(18)	0.0047(9)	0.052(10)	0.054(11)
2585	0.44(11)	0.76(18)	0.0038(9)	0.042(10)	0.044(11)
2594	7.30(57)	17.28(113)	0.0855(56)	0.946(62)	0.990(64)
2604	1.33(14)	4.26(43)	0.0208(21)	0.230(23)	0.241(24)
2645	0.64(17)	1.17(30)	0.0055(14)	0.061(16)	0.063(16)
2666	1.57(20)	2.90(37)	0.0132(17)	0.146(19)	0.153(19)
2680	7.61(59)	30.46(159)	0.1357(71)	1.512(79)	1.582(82)
2695	2.19(22)	4.14(41)	0.0183(18)	0.202(20)	0.212(21)
2698	0.69(15)	1.30(28)	0.0057(12)	0.063(13)	0.066(14)
2706	1.05(13)	4.25(42)	0.0185(18)	0.205(20)	0.214(21)
2747	5.52(45)	10.84(88)	0.0452(37)	0.499(40)	0.523(42)
2762	13.78(106)	27.36(210)	0.1122(86)	1.241(95)	1.298(100)
2801	1.71(16)	9.08(74)	0.0357(29)	0.395(32)	0.413(34)
2854	1.99(19)	6.78(64)	0.0252(24)	0.279(26)	0.292(27)
2866	0.62(11)	1.32(23)	0.0049(8)	0.054(9)	0.056(10)
2911	0.80(12)	1.76(27)	0.0062(10)	0.068(11)	0.071(11)
2919	0.48(12)	1.07(28)	0.0037(10)	0.041(11)	0.043(11)
2923	0.80(13)	4.48(57)	0.0155(20)	0.171(22)	0.179(23)
2944	0.91(15)	2.04(35)	0.0069(12)	0.076(13)	0.080(14)
2956	1.82(18)	4.13(40)	0.0138(13)	0.153(15)	0.160(15)

TABLE I. (*Continued*).

E [keV]	$I_{S,0}$ [eV b]	$g\Gamma_0$ [meV]	$B(M1)\uparrow$ [μ_N^2]	$B(E1)\uparrow$ [10^{-3} e^2 fm^2]	$g\Gamma_0^{\mathrm{red}}$ [meV]/[MeV^3]
2960	0.77(12)	1.75(27)	0.0058(9)	0.064(10)	0.067(10)
2966	0.64(13)	1.46(31)	0.0048(10)	0.053(11)	0.056(12)
2991	0.89(12)	2.07(27)	0.0067(9)	0.074(10)	0.077(10)
3028	1.08(14)	2.58(33)	0.0080(10)	0.089(12)	0.093(12)
3056	0.66(11)	1.61(26)	0.0049(8)	0.054(9)	0.056(9)
3082	0.54(12)	3.58(67)	0.0106(20)	0.117(22)	0.122(23)
3108	0.55(15)	1.38(38)	0.0040(11)	0.044(12)	0.046(13)
3114	0.73(11)	1.84(28)	0.0053(8)	0.058(12)	0.061(9)
3138	0.92(15)	2.37(37)	0.0066(10)	0.073(12)	0.077(12)
3153	3.55(29)	12.40(88)	0.0342(24)	0.378(27)	0.396(28)
3165	0.55(10)	1.45(27)	0.0039(7)	0.044(8)	0.046(8)
3201	0.50(13)	2.29(54)	0.0060(14)	0.067(16)	0.070(17)
3223	0.95(15)	4.89(57)	0.0126(15)	0.140(16)	0.146(17)
3242	0.50(11)	2.93(56)	0.0074(15)	0.082(16)	0.086(17)
3288	0.83(12)	2.34(35)	0.0057(8)	0.063(9)	0.066(10)
3296	2.89(25)	11.48(87)	0.0277(21)	0.306(23)	0.321(24)
3315	1.36(16)	3.90(46)	0.0092(11)	0.102(12)	0.107(13)
3331	2.81(25)	12.05(86)	0.0282(20)	0.312(22)	0.326(23)
3339	1.34(15)	3.88(45)	0.0090(10)	0.100(11)	0.104(12)
3345	0.78(12)	4.40(65)	0.0102(15)	0.112(17)	0.118(17)
3358	0.54(14)	1.57(40)	0.0036(9)	0.040(10)	0.041(11)
3401	0.56(12)	1.69(36)	0.0037(8)	0.041(9)	0.043(9)
3411	0.59(12)	1.78(36)	0.0039(8)	0.043(9)	0.045(9)
3435	0.85(15)	2.60(47)	0.0055(10)	0.061(11)	0.064(12)
3440	1.06(17)	5.40(69)	0.0115(15)	0.127(16)	0.133(17)
3449	0.88(20)	2.72(61)	0.0057(13)	0.063(14)	0.066(15)
3462	0.79(14)	4.52(78)	0.0094(16)	0.104(18)	0.109(19)
3521	1.01(19)	3.27(61)	0.0065(12)	0.072(13)	0.075(14)
3531	1.38(23)	4.48(74)	0.0088(15)	0.097(16)	0.102(17)
3535	1.24(22)	4.04(73)	0.0079(14)	0.087(16)	0.092(17)
3557	0.64(13)	2.12(44)	0.0041(8)	0.045(9)	0.047(10)
3573	1.27(19)	6.42(90)	0.0122(17)	0.135(19)	0.141(20)
3589	2.29(25)	11.93(137)	0.0223(26)	0.247(28)	0.258(30)
3600	0.69(14)	2.32(46)	0.0043(9)	0.047(9)	0.050(10)
3613	1.63(21)	5.55(72)	0.0102(13)	0.112(15)	0.118(15)
3617	1.41(24)	4.82(83)	0.0088(15)	0.097(17)	0.102(18)
3652	1.92(38)	6.65(131)	0.0118(23)	0.130(26)	0.137(27)
3660	0.91(16)	3.16(57)	0.0056(10)	0.062(11)	0.065(12)
3691	1.43(22)	5.08(79)	0.0087(14)	0.096(15)	0.101(16)
3708	0.91(28)	3.26(99)	0.0055(17)	0.061(19)	0.064(19)
3728	1.35(26)	4.88(96)	0.0081(16)	0.090(18)	0.094(18)
3773	1.06(20)	3.93(73)	0.0063(12)	0.070(13)	0.073(14)
3790	0.85(19)	3.18(73)	0.0051(12)	0.056(13)	0.058(13)
3798	1.06(19)	3.99(71)	0.0063(11)	0.070(12)	0.073(13)
3820	1.79(26)	28.12(226)	0.0436(35)	0.482(39)	0.504(40)
3831	1.65(25)	6.30(95)	0.0097(15)	0.107(16)	0.112(17)
3890	1.86(36)	7.33(142)	0.0108(21)	0.119(23)	0.124(24)
3904	1.02(24)	4.06(95)	0.0059(14)	0.065(15)	0.068(16)
3916	1.71(33)	6.82(133)	0.0098(19)	0.109(21)	0.114(22)
3936	1.99(33)	8.03(132)	0.0114(19)	0.126(21)	0.132(22)
3944	0.94(29)	3.80(117)	0.0053(16)	0.059(18)	0.062(19)
3977	1.87(33)	7.71(136)	0.0106(19)	0.117(21)	0.123(22)

[a]Branching $\Gamma_0/\Gamma = 0.75$ taken from the literature [2].

TABLE II. Integrated cross sections $I_{S,0}$, $I_{S,1}$, and $I_{S,2}$ for transitions to the ground state, and the excited levels at $E_1=295.0$ keV and $E_2=357.4$ keV, respectively, together with the corresponding branching ratios $R_{1,0}^{\mathrm{expt}}$ and $R_{2,0}^{\mathrm{expt}}$.

E_x [keV]	$I_{S,0}$ [eV b]	$I_{S,1}$ [eV b]	$I_{S,2}$ [eV b]	$R_{1,0}^{\mathrm{expt}}$	$R_{2,0}^{\mathrm{expt}}$
1923	1.98(22)	1.1(2)		0.93(22)	
1969	5.92(45)	2.0(2)	1.8(4)	0.56(8)	0.55(12)
2128	4.64(36)	2.7(4)		0.92(14)	
2155	2.17(24)	3.1(3)		2.26(34)	
2468	1.09(21)		1.1(2)		1.65(41)
2516	0.58(12)		1.6(3)		4.31(113)
2594	7.30(57)	2.6(3)		0.50(17)	
2604	1.33(14)	1.1(2)		1.17(25)	
2680	7.61(59)	6.9(5)	1.7(3)	1.30(14)	0.35(6)
2706	1.05(13)		1.2(2)		1.71(33)
2801	1.71(16)	1.2(2)	1.6(2)	0.96(21)	1.37(24)
2854	1.99(19)	1.2(2)		0.84(18)	
2923	0.80(13)	1.2(2)		2.11(52)	
3082	0.54(12)	0.9(2)		2.26(79)	
3153	3.55(29)	1.2(2)		0.47(8)	
3201	0.50(13)	0.4(2)		0.97(49)	
3223	0.95(15)		0.9(1)		1.29(30)
3242	0.50(11)	0.6(2)		1.53(59)	
3296	2.89(25)	1.2(2)		0.53(9)	
3331	2.81(25)	1.4(2)		0.64(10)	
3345	0.78(12)	0.7(2)		1.22(37)	
3440	1.06(17)	0.7(1)		0.86(23)	
3462	0.79(14)		0.7(2)		1.17(42)
3573	1.27(19)	0.7(2)		0.68(22)	
3589	2.29(25)		1.3(3)		0.76(21)
3820	1.79(26)	4.2(5)	1.5(3)	2.96(55)	1.09(25)

$\pm 1.9)$ meV/MeV^3 corresponding, under the assumption of an electric character for all excitations, to a total excitation strength of $\Sigma_{2-4\ \mathrm{MeV}}\ B(E1)\uparrow=(15.6\pm 1.8)\times 10^{-3}\ e^2\ \mathrm{fm}^2$.

This value has to be compared with the observations for other odd-mass nuclei in the neighboring mass regions. In the vibrational odd-mass nucleus ^{113}Cd [30] a somewhat reduced total dipole strength of $\Sigma_{2-4\ \mathrm{MeV}}\ g\Gamma_0^{\mathrm{red}}=(8.5\pm 1.7)$ meV/MeV^3 was observed which amounts to about 3/4 of that observed in the neighboring even-even isotopes ^{112,114}Cd [30,31]. In the semimagic, spherical, odd-mass nucleus ^{117}Sn in the same range of excitation energies a total dipole strength of $\Sigma_{2-4\ \mathrm{MeV}}\ g\Gamma_0^{\mathrm{red}}=(11.6\pm 1.3)$ meV/MeV^3 was found [26,27]. In this case of a semimagic nucleus microscopic calculations within the framework of the quasiparticle-phonon model (QPM) succeeded to show that even if the electric dipole excitations ($E1$) are the strongest ones, also magnetic dipole ($M1$) and electric quadrupole excitations ($E2$) contribute substantially to the observed spectra. This shows that some caution seems to be appropriate when comparing the dipole strengths distributions observed in odd-mass nuclei of different masses and shapes. For example, in a recent high sensitivity NRF experiment [21] on the well-deformed nucleus ^{165}Ho a huge total dipole strength of $\Sigma_{2-4\ \mathrm{MeV}} g\Gamma_0^{\mathrm{red}}=(36.1\pm 4.0)$ meV/MeV^3 was detected. However, in the case of well-deformed nuclei it is

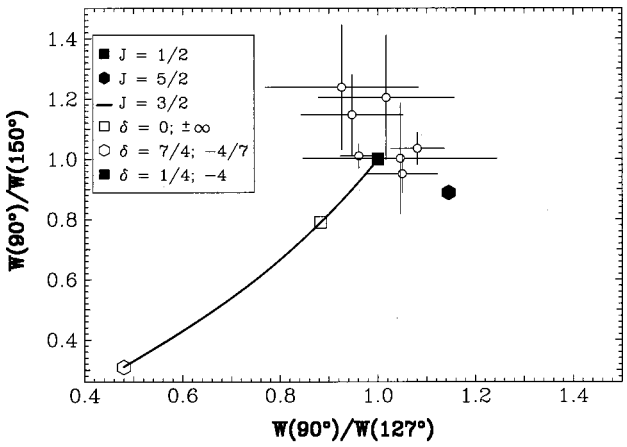

FIG. 3. Plot of angular distribution ratios $W(90°)/W(150°)$ versus $W(90°)/W(127°)$ for levels with a tentative spin assignment $J=1/2$, corresponding to an isotropic angular distribution (shown as a full square). The full line gives the values expected for $J=3/2$ levels as a function of the mixing ratio δ. The values for extreme mixing ratios δ are given and explained in the inset. The value for pure $E2$ excitations ($J=5/2$) is shown as a full hexagon.

well known that the overwhelming fraction of the low-lying dipole strength observed in NRF experiments should be attributed to magnetic dipole excitations of the scissors mode [12] (see, e.g., Ref. [13], and references therein) which, on the other hand, in odd-mass nuclei can be extremely fragmented [17,18,20,21]. Therefore, the detected dipole strength strongly depends on the experimental sensitivity. This is also

TABLE III. Numerical results of the angular distribution measurements: Excitation energies E_x, intensity ratios $W(90°)/W(127°)$, and $W(90°)/W(150°)$ for ground-state transitions and tentative spin asignments.

E_x [keV]	$W(90)°/W(127)°$	$W(90)°/W(150)°$	Spin assignment
1277	0.84(24)	0.52(12)	3/2
1861	0.93(16)	1.24(21)	1/2, 3/2, (5/2)
1969	1.05(7)	0.95(6)	1/2, 3/2
2128	1.14(9)	1.25(9)	(1/2) ?
2319	0.77(21)	0.76(20)	3/2, 1/2, (5/2)
2594	1.16(6)	1.19(6)	(1/2) ?
2680	1.08(6)	1.04(5)	1/2, 3/2
2695	1.00(17)	0.85(13)	3/2, 5/2, 1/2
2706	0.87(23)	0.84(21)	3/2, 1/2, 5/2
2747	0.85(6)	0.72(5)	3/2
2762	0.96(4)	1.01(4)	1/2, 3/2
2801	1.02(16)	0.81(12)	3/2, 5/2, 1/2
2854	1.02(14)	1.20(21)	1/2, 3/2, 5/2
2956	0.89(14)	0.82(12)	3/2, 1/2, (5/2)
3223	0.58(19)	0.64(26)	3/2
3296	1.00(11)	0.95(10)	1/2, 3/2, 5/2
3331	0.95(10)	1.15(13)	1/2, 3/2, 5/2
3339	0.73(16)	0.81(19)	3/2, 1/2
3589	1.05(20)	1.00(18)	1/2, 3/2, 5/2
3820	0.67(22)	0.66(22)	3/2, 1/2

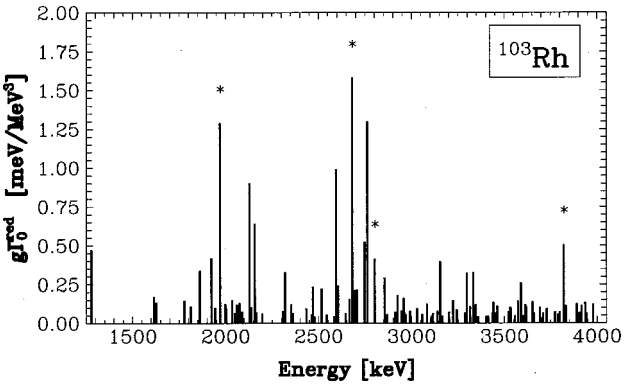

FIG. 4. Dipole strength distribution in ^{103}Rh. Plotted are the observed reduced ground-state decay widths Γ_0^{red} as a function of the excitation energy. Bars marked by asterisks correspond to the excitation of levels which feed the two levels of interest at 357 and 295 keV, respectively. ($g\Gamma_0^{\mathrm{red}}=1$ meV/MeV^3 corresponds to $B(E1)\uparrow=0.955\times10^{-3}\ e^2\ \mathrm{fm}^2$).

documented by the fact that, e.g., the strengths in odd-mass deformed rare earth nuclei, detectable in present day NRF experiments, decreases in lighter rare earth nuclei steadily towards lower mass numbers A and reaches in ^{151}Eu a minimal value of only $\Sigma_{2-4\ \mathrm{MeV}}\ g\Gamma_0^{\mathrm{red}}\approx 1.5$ meV/MeV^3 [21]. Nevertheless, recent fluctuation analyses of the measured photon scattering spectra [22,23] demonstrated that a part of the strength is hidden in the continuous background of the spectra of scattered photons and that the total $M1$ strength in odd-mass deformed rare earth nuclei corresponds to that observed in the neighboring even-even nuclei and as expected from sum rule predictions [40–44]. Furthermore, in recent improved NRF experiments of considerably increased sensitivity on ^{163}Dy and ^{165}Ho [21] it could be shown experimentally that nearly the complete expected total $M1$ strength is existent in odd-mass nuclei too.

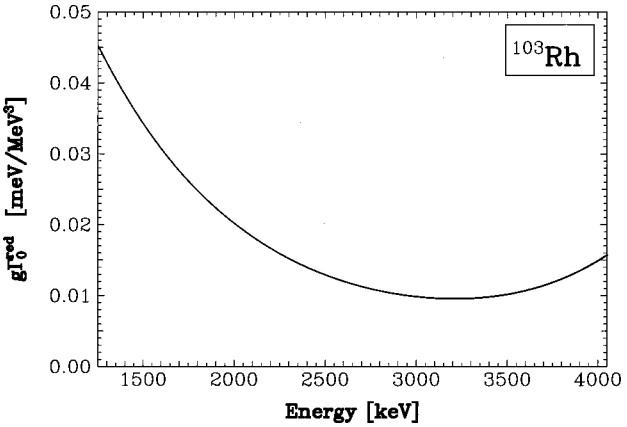

FIG. 5. Detection limits in the present photon scattering experiments (bremsstrahlung endpoint energy 4.1 MeV): plotted is the minimal reduced ground-state transition width Γ_0^{red} times the spin factor g as a function of the excitation energy, needed for levels to be detected in the present experiments. [$g\Gamma_0^{\mathrm{red}}=0.01$ meV/MeV^3 corresponds to $B(E1)\uparrow=0.955\times10^{-5}\ e^2\ \mathrm{fm}^2$ or $B(M1)\uparrow=0.864\times10^{-2}\ \mu_N^2$].

TABLE IV. Properties of photoexcited states populating both low-lying states at 295 and 357 keV, respectively. Excitation energies, total ground-state scattering intensities $I_{S,0}$, decay branching ratios $R_{1,0}^{\mathrm{expt}}$ and $R_{2,0}^{\mathrm{expt}}$, the relative feeding $R_{2,0}^{\mathrm{expt}}/R_{1,0}^{\mathrm{expt}}$, and probable spins J of the photoexcited feeding levels are given.

E_x [keV]	$I_{S,0}$ [eVb]	$R_{2,0}^{\mathrm{expt}}$	$R_{1,0}^{\mathrm{expt}}$	$R_{2,0}^{\mathrm{expt}}/R_{1,0}^{\mathrm{expt}}$	J
1969	5.92(45)	0.55(12)	0.56(8)	0.98(26)	1/2; (3/2)
2680	7.61(59)	0.35(6)	1.30(14)	0.27(8)	1/2; 3/2
2801	1.71(16)	1.37(24)	0.96(21)	1.43(40)	3/2; 1/2
3820	1.79(26)	1.09(25)	2.96(55)	0.37(11)	3/2; (1/2)

B. Decay branching ratios

In Table IV the properties of the four photoexcited levels are summarized which exhibit strong feedings to both low-lying levels at 295 keV ($J^\pi=3/2^-$) and 357 keV ($J^\pi=5/2^-$). In addition to the decay branching ratios $R_{1,0}^{\mathrm{expt}}$ and $R_{2,0}^{\mathrm{expt}}$ [see Eq. (6)], the relative feedings $R_{2,0}^{\mathrm{expt}}/R_{1,0}^{\mathrm{expt}}$ are given together with the probable spin assignments as suggested from the measured angular distributions (see Table III). Unfortunately, the observed decay branching ratios do not provide further constraints for the suggested spin assignments since the applicability of the Alaga rules [38] seems to be rather questionable in the case of a not well deformed nucleus such as ^{103}Rh.

Whereas the states at 2680 and 3820 keV predominantly populate the level at 295 keV, the states at 1969 and 2801 keV show an enhanced feeding of the higher-lying level at 357 keV. Such a decay pattern favors the generation of an inversion, the basic requirement for a γ-ray laser. Since, in addition, the lifetime of the 357 keV level is considerably longer than that of the lower-lying 295 keV state (107 ps compared to 9.7 ps) a population inversion of nuclear states by feeding from higher-lying photoexcited states could be demonstrated by the present experiments. In particular the lowest observed state at 1969 keV seems to be a good candidate for such a pumping scheme due to its lower excitation energy and its strong excitation cross section.

C. Population inversion between the 357 and 295 keV states

To calculate the inversion between the 357 and 295 keV levels, the steady-state rate equations for the population in the two level are solved and a summation is made of the contribution of all feeding levels which decay to the upper or lower laser level or to both [36]. This yields

$$\Delta N=N_g\sum_f n_p\sigma_f[F_u\tau_u-(3/2)F_l\tau_l], \tag{7}$$

where N_g is the population density of the ground level (equal to the number of atoms per cm^3 of solid rhodium), n_p is the number of pump photons per (s eV cm^2). σ_f is the integrated absorption cross section of the feeding level from the ground state (in cm^2 eV), and $\tau_{u,l}$ are the lifetimes of the upper and lower laser levels, respectively; the quantities $F_{u,l}$ are the ratios of the radiative decay rates given by $F_u=A_{fu}/(A_{fu}$

$+A_{fg}$) and $F_u = A_{fl}/(A_{fl}+A_{fg})$ where A_{ik} denotes the Einstein A coefficient of spontaneous emission on the i-k transition and the subscripts f, u, l, and g denote the feeding, upper, and lower laser levels, and the ground state. The factor 3/2 in Eq. (7) is the ratio of the statistical weights of the upper and lower levels.

Making the summation with the measured branching ratios and the excitation cross sections from the ground state taken into account, we find that inversion between the 357.4 and 295.0 keV levels in ^{103}Rh is indeed generated. With the photon flux distribution applied to the sample the calculated inversion density is $\Delta N = (6.9 \pm 1.8) \times 10^{-8}$ cm^{-3}.

The value of the inversion density obtained by feeding has to be corrected for the effect of direct excitation of the lasing levels. This effect can be estimated by taking into account the photon flux for direct excitation (i.e., at 357.4 and 295.0 keV) and the integrated cross sections $\sigma_{u,l}$ for excitation of the upper and lower levels from the ground state, which are given by

$$\sigma_{u,l} = \frac{\lambda_{u,l}^2 A_{u,l}}{8\pi} g_{u,l}. \tag{8}$$

Here $A_{u,l}$ are the Einstein A coefficients of the transitions to the ground state, $\lambda_{u,l}$ are the respective wavelengths. The statistical weight g_u is 3 for the upper and $g_l = 2$ for the lower level. After this correction, the inversion density is found to be reduced by only 25%, even though the photon flux for a direct excitation is about 20 times higher than that for the excitation of the feeding levels. This relatively low reduction is due to the small cross section for a direct excitation, a result of the magnetic dipole and electric quadrupole character of the transitions.

We note that the stimulated emission cross section can be estimated to be of the order 10^{-21} cm^2 and thus the generated inversion is much too small to result in experimentally measurable gain. Pulsed excitation with high photon fluxes (for example from a laser plasma) will be necessary to achieve higher inversion and gain. These aspects of the present experiments will be discussed in more detail in a forthcoming article [35].

ACKNOWLEDGMENTS

The support by the Deutsche Forschungsgemeinschaft under Contract Nos. Br 799/6, Kn 154/30, and partially Pi 393/1 is gratefully acknowledged.

[1] A. Bohr and B.R. Mottelson, *Nuclear Structure* (Benjamin, Reading, MA, 1975), Vol. II.
[2] *Table of Isotopes*, edited by R.B. Firestone and V.S. Shirley (Wiley, New York, 1996), Vol. I.
[3] N.P. Heydenburg and G.M. Temmer, Phys. Rev. **95**, 861 (1954).
[4] A. Gelberg, B. Herskind, R. Kalish, and M. Neiman, Z. Phys. A **279**, 183 (1976).
[5] A. Arima and F. Iachello, Phys. Rev. Lett. **35**, 1069 (1975).
[6] R.O. Sayer, J.K. Temperley, and D. Eccleshall, Nucl. Phys. **A179**, 122 (1972).
[7] Chr. Bargholtz, J. Becker, L. Eriksson, L. Holmberg, and V. Stefánsson, Phys. Scr. **8**, 90 (1973).
[8] K. Heyde and P.J. Brussard, Nucl. Phys. **A104**, 81 (1967).
[9] B. Castel, K.W.C. Stewart, and M. Harvey, Nucl. Phys. **A162**, 273 (1971).
[10] *Table of Isotopes*, edited by R.B. Firestone and V.S. Shirley (Wiley New York, 1996), Vol. II.
[11] A. Leprêtre, H. Beil, R. Bergère, P. Carlos, A. De Miniac, and A. Veyssière, Nucl. Phys. **A219**, 39 (1974).
[12] D. Bohle, A. Richter, W. Steffen, A.E.L. Dieperink, N. Lo Iudice, F. Palumbo, and O. Scholten, Phys. Lett. **137B**, 27 (1984).
[13] U. Kneissl, H.H. Pitz, and A. Zilges, Prog. Part. Nucl. Phys. **37**, 349 (1996).
[14] R.-D. Herzberg, I. Bauske, P. von Brentano, Th. Eckert, R. Fischer, W. Geiger, U. Kneissl, J. Margraf, H. Maser, N. Pietralla, H.H. Pitz, and A. Zilges, Nucl. Phys. **A592**, 211 (1995), and references therein.
[15] J. Bryssinck, L. Govor, D. Belic, F. Bauwens, O. Beck, P. von Brentano, D. De Frenne, T. Eckert, C. Fransen, K. Govaert, R.-D. Herzberg, E. Jacobs, U. Kneissl, H. Maser, A. Nord, N. Pietralla, H.H. Pitz, V.Yu. Ponomarev, and V. Werner, Phys. Rev. C **59**, 1930 (1999).
[16] I. Bauske, J.M. Arias, P. von Brentano, A. Frank, H. Friedrichs, R.D. Heil, R.-D. Herzberg, F. Hoyler, P. Van Isacker, U. Kneissl, J. Margraf, H.H. Pitz, C. Wesselborg, and A. Zilges, Phys. Rev. Lett. **71**, 975 (1993).
[17] J. Margraf, T. Eckert, M. Rittner, I. Bauske, O. Beck, U. Kneissl, H. Maser, H.H. Pitz, A. Schiller, P. von Brentano, R. Fischer, R.-D. Herzberg, N. Pietralla, A. Zilges, and H. Friedrichs, Phys. Rev. C **52**, 2429 (1995).
[18] A. Nord, A. Schiller, T. Eckert, O. Beck, J. Besserer, P. von Brentano, R. Fischer, R.-D. Herzberg, D. Jäger, U. Kneissl, J. Margraf, H. Maser, N. Pietralla, H.H. Pitz, M. Rittner, and A. Zilges, Phys. Rev. C **54**, 2287 (1996).
[19] C. Schlegel, P. von Neumann-Cosel, A. Richter, and P. Van Isacker, Phys. Lett. B **375**, 21 (1996).
[20] N. Huxel, P. von Brentano, J. Eberth, J. Enders, R.-D. Herzberg, P. von Neumann-Cosel, N. Nicolay, N. Pietralla, H. Prade, C. Rangacharyulu, J. Reif, A. Richter, C. Schlegel, R. Schwengner, S. Skoda, H.G. Thomas, I. Wiedenhöver, G. Winter, and A. Zilges, Nucl. Phys. **A645**, 239 (1999).
[21] A. Nord, Ph.D. thesis, University of Stuttgart, 2000.
[22] J. Enders, N. Huxel, P. von Neumann-Cosel, and A. Richter, Phys. Rev. Lett. **79**, 2010 (1997).
[23] J. Enders, N. Huxel, U. Kneissl, P. von Neumann-Cosel, A. Richter, and H.H. Pitz, Phys. Rev. C **57**, 996 (1998).
[24] A. Zilges, R.-D. Herzberg, P. von Brentano, F. Dönau, R.D. Heil, R.V. Jolos, U. Kneissl, J. Margraf, H.H. Pitz, and C.

Wesselborg, Phys. Rev. Lett. **70**, 2880 (1993).
[25] R.-D. Herzberg, A. Zilges, A. M. Oros, P. von Brentano, U. Kneissl, J. Margraf, H. H. Pitz, and C. Wesselborg, Phys. Rev. C **51**, 1226 (1995).
[26] V.Yu. Ponomarev, J. Bryssinck, L. Govor, F. Bauwens, O. Beck, D. Belic, P. von Brentano, D. De Frenne, C. Fransen, R.-D. Herzberg, E. Jacobs, U. Kneissl, H. Maser, A. Nord, N. Pietralla, H.H. Pitz, and V. Werner, Phys. Rev. Lett. **83**, 4029 (1999).
[27] J. Bryssinck, L. Govor, V.Yu. Ponomarev, F. Bauwens, O. Beck, D. Belic, P. von Brentano, D. De Frenne, C. Fransen, R.-D. Herzberg, E. Jacobs, U. Kneissl, H. Maser, A. Nord, N. Pietralla, H.H. Pitz, and V. Werner, Phys. Rev. C **62**, 014309 (2000).
[28] H. Maser, N. Pietralla, P. von Brentano, R.-D. Herzberg, U. Kneissl, J. Margraf, H.H. Pitz, and A. Zilges, Phys. Rev. C **54**, R2129 (1996).
[29] J. Besserer, O. Beck, P. von Brentano, T. Eckert, R.-D. Herzberg, D. Jäger, U. Kneissl, J. Margraf, H. Maser, A. Nord, N. Pietralla, H.H. Pitz, and A. Zilges, Phys. Rev. C **56**, 1276 (1997).
[30] W. Geiger, Zs. Németh, I. Bauske, P. von Brentano, R.D. Heil, R.-D. Herzberg, U. Kneissl, J. Margraf, H. Maser, N. Pietralla, H.H. Pitz, C. Wesselborg, and A. Zilges, Nucl. Phys. **A580**, 263 (1994).
[31] H. Lehmann, A. Nord, A.E. de Almeida Pinto, O. Beck, J. Besserer, P von Brentano, S. Drissi, T. Eckert, R.-D. Herzberg, D. Jäger, J. Jolie, U. Kneissl, J. Margraf, H. Maser, N. Pietralla, and H.H. Pitz, Phys. Rev. C **60**, 024 308 (1999).
[32] Y. Cauchois, H. Ben Abdelaziz, K. Khérouf, and C. Schloessing-Möller, J. Phys. G **7**, 1593 (1981).
[33] C.B. Collins, F.W. Lee, D.M. Shemwell, B.D. DePaola, S. Olariu, and I. Iovitzu Popescu, J. Appl. Phys. **53**, 4645 (1982).
[34] C.B. Collins and J.J. Carroll, Hyperfine Interact. **107**, 3 (1997).
[35] F. Stedile, Diploma thesis, University of Stuttgart, 2000; E. Fill *et al.* (unpublished).
[36] F. Stedile, D. Belic, E. Fill, P. von Brentano, C. Fransen, U. Kneissl, Ch. Kohstall, A. Linnemann, P. Matschinsky, A. Nord, N. Pietralla, H.H. Pitz, M. Scheck, and V. Werner, Proceedings of the 7th International Conference on ''X-Ray Lasers'' (XRL2000), Saint Malo, France, 2000 (to be published).
[37] U.E.P. Berg and U. Kneissl, Annu. Rev. Nucl. Part. Sci. **37**, 33 (1987).
[38] G. Alaga, K. Alder, A. Bohr, and B.R. Mottelson, Dokl. Akad. Nauk SSSR **29**, 1 (1955).
[39] N. Pietralla, I. Bauske, O. Beck, P. von Brentano, W. Geiger, R.-D. Herzberg, U. Kneissl, J. Margraf, H. Maser, H.H. Pitz, and A. Zilges, Phys. Rev. C **51**, 1021 (1995).
[40] P. van Isacker, K. Heyde, J. Jolie, and A. Sevrin, Ann. Phys. (N.Y.) **171**, 253 (1986).
[41] J.N. Ginocchio, Phys. Lett. B **265**, 6 (1991).
[42] N. Lo Iudice and A. Richter, Phys. Lett. B **304**, 193 (1993).
[43] P. von Neumann-Cosel, J.N. Ginocchio, H. Bauer, and A. Richter, Phys. Rev. Lett. **75**, 4178 (1995).
[44] N. Lo Iudice, Phys. Rev. C **53**, 2171 (1996).